Korean J. Chem. Eng., 33(11), 3069-3078 (2016)
DOI: 10.1007/s11814-016-0229-9
pISSN: 0256-1115
eISSN: 1975-7220

REVIEW PAPER

A review on particle dynamics simulation techniques for colloidal dispersions: Methods and applications

Jun Dong Park*, Jin Suk Myung, and Kyung Hyun Ahn*,†**

*School of Chemical and Biological Engineering, Institute of Chemical Process, Seoul National University, Seoul 08826, Korea
**Physical Chemistry, Department of Chemistry, Lund University, SE-22100 Lund, Sweden
(*Received 2 July 2016 • accepted 7 August 2016*)

Abstract−Colloidal dispersions have attracted much attention both from academia and industry due to industrial significance and complex dynamic properties. Accordingly, a variety of attempts have been made to understand the complicated physics of colloidal dispersions. Particle dynamics simulation has been playing an important role in exploring colloidal systems as a strong complement to experimental approaches from which it is hard to get exact microscopic information. Our aim is to provide a well-organized and up-to-date guide to particle dynamics simulation of colloidal dispersions. Among diverse particle dynamics simulation techniques, we focus on Brownian dynamics, Stokesian dynamics, multi-particle collision dynamics, and self-consistent particle simulation techniques. First, the concept of the simulation techniques will be described. Then, for each simulation technique, pros and cons are discussed with a broad range of applications, including concentrated hard sphere suspensions and biological systems. It is expected that this article helps to identify and motivate research challenges.

Keywords: Particle Dynamics Simulation, Brownian Dynamics, Stokesian Dynamics, Multi-particle Collision Dynamics, Self-consistent Particle Simulation

INTRODUCTION

Colloidal systems have attracted much attention from both academia and industry because of their rich phase behavior and mechanical properties. Colloidal dispersion refers to a particle system with a length scale that is larger than molecular length scale, but small enough to be affected by thermal fluctuation and interparticle forces such as van der Waals force and electrostatic force [1-3]. Typically, particles with effective diameter on the order of tens of nanometer to several microns fall under this colloidal regime. Depending on the flow conditions, concentration, and particle interactions, they demonstrate characteristic microstructure and dynamics, which are closely related to physical properties such as electrical and rheological properties. From the academic perspective, the primary goal of exploring colloidal dispersions is to understand the microstructure and dynamics. From an application perspective, the understanding on colloidal dispersions can be usefully employed in controlling the properties and performance of the product.

There have been various approaches to studying colloidal systems. A typical example is experimental approaches using scattering techniques such as small angle neutron scattering (SANS) [4,5] and wide angle X-ray scattering (WAXS) [6]. Lately, direct visualization techniques using confocal microscopy have also been employed [7,8]. Rheometry is another commonly used experimental methodology. However, these experimental approaches have limitations with regard to sample conditions such as volume fraction, length scales, and time scales. In addition, as the colloidal dispersions of interest become more complicated with diverse performances (e.g., complex particle shapes, polydispersity, etc.), experimental approaches have limits in obtaining enough information and interpreting the result. As an alternative, theoretical approaches using particle dynamics simulation have been suggested. Taking the advantage that enables easy investigation on particle position and dynamics, particle dynamics simulation has played a role as a standalone methodology and sometimes as an additional tool to aid experimental study.

Our aim is to provide a simple review on particle dynamics simulation techniques for colloidal dispersions. As the field of the particle dynamics simulation is fairly large, we cannot deal with all techniques in this work. Therefore, excluding several techniques, such as Lattice-Boltzmann technique, we will focus on off-lattice Lagrangian particle dynamics simulation methods where the particles are treated explicitly. Four kinds of particle dynamics simulations (Brownian dynamics, Stokesian dynamics, multi-particle collision dynamics, self-consistent particle simulation) are selected to be discussed. At the beginning of each part, implementation of each simulation technique is described briefly and to the point. Thereafter, a wide range of application cases are introduced, and the pros and cons of each technique are discussed. Lastly, in conclusion, we compare and assess the four different techniques altogether in various aspects.

BROWNIAN DYNAMICS (BD)

1. BD Implementation

The dynamics of a sphere particle suspended in a medium is

†To whom correspondence should be addressed.
E-mail: ahnnet@snu.ac.kr

governed by a momentum balance. The particles experience collision with atoms or molecules of the medium. The collision makes particles move in a random way. This irregular motion is well known as Brownian motion, and a particle moving with this random motion is called as a Brownian particle [9]. The Brownian force from the solvent molecules plays an important role in determining the physics of dispersions. For example, stability, internal structure, and rheological properties can be significantly affected by the Brownian motion [10-12]. For a Brownian particle, there is another effect of fluid medium: the viscous friction acting against particle motion. The viscous drag can be described by Stokes equation on time scales relatively longer than viscous relaxation. Additionally, there can be external forces induced by other particles. Putting all these together, the viscous drag, the Brownian force, and the external forces should balance particle inertia such that

$$m\frac{d\mathbf{v}_i}{dt}=\sum_j \mathbf{F}_{ij}(\mathbf{r}_{ij})+\mathbf{F}_i^{B}+\mathbf{F}_i^{D} \tag{1}$$

with m, the mass of Brownian particle, and $\mathbf{v}_i$, the particle velocity. Eq. (1) is called Langevin equation [1,2,13]. The first term on the right hand side $\mathbf{F}_{ij}(\mathbf{r}_{ij})$ indicates the inter-particle force exerted on *i*-particle due to *j*-particle at separation $\mathbf{r}_{ij}$. The second term $\mathbf{F}_i^{B}$ and third term $\mathbf{F}_i^{D}$ represent Brownian force and viscous drag force, respectively.

The inter-particle interaction $\mathbf{F}_{ij}(\mathbf{r}_{ij})$ has been described in various ways by using a number of inter-particle potentials according to its origin. In the case of hard spheres, interparticle interaction is described by repulsive hard core interaction which arises from the overlap of particle surfaces [14-16]. Recently, a new technique, called potential free method, has been developed to model the inter-particle interaction between hard spheres [17,18]. Interaction between soft spheres that interact through attractive or repulsive force is more complicated. For soft sphere particles interacting through electrostatic force and van der Waals force, Derjaguin-Landau-Verwey-Overbeek (DLVO) potential works effectively [2,19,20]. Depletion attraction is another typical attractive interaction induced by an effect of increased osmotic pressure in the surrounding medium and can be properly described by Asakura-Oosawa model [20-22]. In addition, there are various potential models such as Lennard-Jones potential and Yukawa potential [15,23,24]. Note that employing adequate potential model is an important factor in particle dynamics simulation.

In the Langevin equation, Brownian motion is expressed through a Brownian force $\mathbf{F}_i^{B}$. The Brownian force is given as a stochastic force characterized by two conditions. First, the Brownian force has random direction and magnitude, which are uncorrelated to each other on the particle motion time scale. Second, kinetic energy is evenly distributed to three translational modes of particles. According to the fluctuation-dissipation theorem [25], these conditions can be described mathematically as

$$\begin{aligned}&\langle \mathbf{F}_i^{B}(t)\rangle=\mathbf{0},\\ &\langle \mathbf{F}_i^{B}(t)\mathbf{F}_i^{B}(t+\tau)\rangle=2k_BT\xi\delta_{ij}\delta(\tau)\delta\end{aligned} \tag{2}$$

where bracket indicates an ensemble average. Here $\delta(\tau)$, δ_{ij}, δ, ξ, and τ represent the Dirac delta function, Kronecker delta, unit second-order tensor, drag coefficient, and arbitrary time difference, respectively. This mathematical description is equivalent to the Fokker-Planck equation [26,27], which delineates the time evolution of the probability density function of a particle with random thermal motion. Generally, the Brownian force is assumed to take the form of Gaussian random distribution with zero mean and variance $2\xi k_BT/\Delta t$ where Δt is the size of the integration time step. This stochastic force gives uncorrelated displacement $\sqrt{2D^T\Delta t}$ for three orthogonal directions (x, y, z) on average, where D^T is the translational diffusion coefficient of a particle at infinite dilution [1,2].

As a particle moves in a fluid, it exerts force on the fluid. As a result of the principle of action and reaction, the particle undergoes dissipative viscous drag force which is noted as $\mathbf{F}_i^{D}$ in the Langevin equation. In Brownian dynamics, the viscous drag force is commonly approximated by a simple Stokesian friction term,

$$\mathbf{F}_i^{D}=-6\pi\eta a(\mathbf{v}_i-\mathbf{u}^{\infty}(\mathbf{r}_i))=-\xi\left(\frac{d\mathbf{r}_i}{dt}-\mathbf{u}^{\infty}(\mathbf{r}_i)\right) \tag{3}$$

where η and a are the viscosity of the fluid medium and the particle radius, respectively. Here, $\mathbf{v}_i$ is the velocity of *i*-th particle and $\mathbf{u}^{\infty}(\mathbf{r}_i)$ is the unperturbed velocity of the fluid medium evaluated at the particle position $\mathbf{r}_i$. The unperturbed velocity field $\mathbf{u}^{\infty}(\mathbf{r}_i)$ can be customized according to the flow condition. For example, in the case of simple shear flow, it takes the form of $(\dot{\gamma}_{xy}y_i, 0, 0)$. However, in the strict sense, the motion of a particle in a fluid medium disturbs the velocity field, which affects the viscous drag force exerted on other particles [28,29]. The interaction through the fluid medium is called the interparticle hydrodynamic interaction and can be influential. Some algorithms suggest an extension to include the effect of the inter-particle hydrodynamic interaction by adopting the concept of diffusion tensor. This will be introduced briefly at the end of this section.

In most cases, the particles have very small mass ($m\rightarrow 0$) and the inertia term on the left hand side of the Langevin equation, Eq. (1), can be neglected. Then, Eq. (1) and Eq. (3) reduce to the following expression:

$$\frac{d\mathbf{r}_i}{dt}=\mathbf{u}^{\infty}(\mathbf{r}_i)+\frac{1}{\xi}\left(\sum_j \mathbf{F}_{ij}(\mathbf{r}_{ij})+\mathbf{F}_i^{B}\right) \tag{4}$$

To calculate the trajectory of each particle, the above stochastic differential equation has to be integrated forward in time. Using an explicit Euler time integration scheme, it can be discretized as follows:

$$\mathbf{r}_i(t+\Delta t)=\mathbf{r}_i(t)+\frac{\Delta t}{\xi}\sum_j \mathbf{F}_{ij}(\mathbf{r}_{ij})+\mathbf{u}^{\infty}(\mathbf{r}_i)\Delta t+\Delta\mathbf{r}_i^{B} \tag{5}$$

As mentioned earlier, the effect of Brownian force $\mathbf{F}_i^{B}$ is manifested as an uncorrelated random displacement $\Delta\mathbf{r}_i^{B}$ which satisfies

$$\begin{aligned}&\langle \Delta\mathbf{r}_i^{B}(t)\rangle=\mathbf{0}\\ &\langle \Delta\mathbf{r}_i^{B}(t)\Delta\mathbf{r}_i^{B}(t+\tau)\rangle=2D^T\Delta t\delta\end{aligned} \tag{6}$$

The position of the particle is updated with the above evolution equation, Eq. (5). With the newly updated information on particle position, the position-dependent physical properties, such as inter-

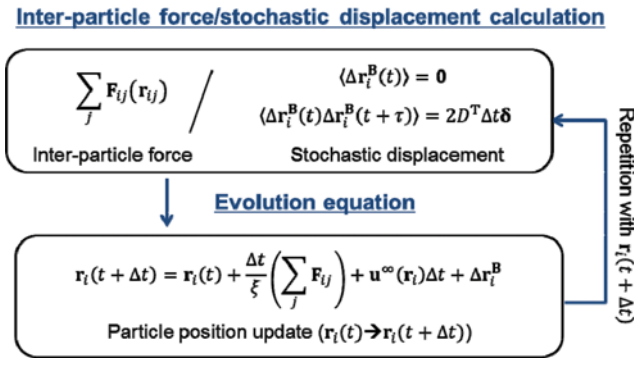

Fig. 1. Algorithm for Brownian dynamics simulation.

particle force $\sum_j \mathbf{F}_{ij}$, are updated and after that, the whole process is repeated. Fig. 1 briefly summarizes the algorithm for BD simulation.

2. BD with Hydrodynamic Interactions

Particle motion in a fluid medium induces disturbances in velocity field. The velocity field disturbance changes the drag force applied to other particles. The medium-mediated interaction, called interparticle hydrodynamic interaction, cannot be considered in classical Brownian dynamics where the viscous drag force is simplified to a Stokesian drag force. As an alternative, extended Brownian dynamics, which includes the effect of hydrodynamic interaction, was suggested [30]. In this algorithm, the effect of inter-particle hydrodynamic interaction is considered through a diffusion tensor $\mathbf{D}_{ij}(\mathbf{r}_i, \mathbf{r}_j)$ given by

$$\mathbf{D}_{ij}(\mathbf{r}_i, \mathbf{r}_j) = \frac{k_B T}{\xi}(\delta_{ij}\delta + \xi \Omega_{ij}(\mathbf{r}_i, \mathbf{r}_j)) \tag{7}$$

Here $\Omega_{ij}(\mathbf{r}_i, \mathbf{r}_j)$ is the hydrodynamic interaction tensor with $\Omega_{ii}=\mathbf{0}$. In particle dynamics simulation, the Oseen tensor and the Rotne-Prager tensor have been widely used [2,31].

The stochastic differential equation for Brownian dynamics with hydrodynamic interaction can be derived as [30]

$$\begin{aligned}\mathbf{r}_i(t+\Delta t) = \mathbf{r}_i(t) + \mathbf{u}^\infty(\mathbf{r}_i)\Delta t + \frac{\Delta t}{k_B T}\sum_j \mathbf{D}_{ij}\mathbf{F}_{ij} \\ + \sum_j \frac{\partial}{\partial \mathbf{r}_j}\cdot \mathbf{D}_{ij} + \sqrt{2}\sum_{j=1}^{N} \mathbf{B}_{ij}\cdot \mathbf{n}_j(t)\end{aligned} \tag{8}$$

where $\mathbf{n}_j(t)$ is a random vector satisfying

$$\begin{aligned}\langle \mathbf{n}_j(t) \rangle &= \mathbf{0} \\ \langle \mathbf{n}_j(t)\mathbf{n}_j(t+\tau) \rangle &= \delta_{ij}\delta(\tau)\delta.\end{aligned} \tag{9}$$

The weighting tensor $\mathbf{B}_{ij}$ is determined from the fluctuation-dissipation theorem [25-27]

$$\mathbf{D}_{ij}(\mathbf{r}_i, \mathbf{r}_j) = \sum_{p=1}^{N} \mathbf{B}_{ip}\cdot \mathbf{B}_{jp}^T \tag{10}$$

To invert the above equation and calculate $\mathbf{B}_{ij}$, Cholesky decomposition or another computationally efficient method can be used [32].

3. Application of BD

Because of relatively low computational cost and expandability, Brownian dynamics has been widely used to explore the physics of various macromolecules and soft matter systems. Studies on colloidal gel and colloidal glass systems are the most typical examples [33-42]. In BD, the effect of interparticle hydrodynamic interaction is simply approximated to Stokesian friction term. This implies that BD cannot describe hydrodynamic interaction correctly. Even though an extended algorithm, as introduced in the previous part, has been suggested to resolve this issue, it is still inadequate to consider the near-field hydrodynamic interaction such as lubrication force. However, despite its inadequacy, BD holds a dominant position in investigating the colloidal gel and colloidal glass systems where the interparticle hydrodynamic interaction is less important. In the case of colloidal gel, the particle dynamics is dominated by nonhydrodynamic inter-particle interaction, such as van der Waals attraction and depletion attraction [43-45]. In addition, the dynamics of the particles that organize a colloidal glass is governed by the excluded volume effect of surrounding particles, often called a cage effect [45-47]. Therefore, without rigorous calculation of the hydrodynamic interaction between the particles, the colloidal gel or colloidal glass system can be reasonably simulated by Brownian dynamics.

One example is the study on the structural evolution of the colloidal gel under start-up shear. It is well known that the colloidal gel under startup shear flow shows nonlinear rheological behavior represented by stress overshoot [48]. Despite many efforts, experimental study alone was not enough to provide a clear explanation on the origin of stress overshoot behavior, because it has limitation in investigating the microstructure. Brownian dynamics, which works effectively for investigation of microstructural change in nonequilibrium state, plays a role as an alternative. BD has successfully reproduced the stress overshoot behavior of the colloidal gel and provided detailed information on the microstructural change that explains the origin of stress overshoot [33]. Lately, BD has expanded the range of application to the study of colloidal gel and glass systems under various flow conditions, such as oscillatory shear flow [34].

Apart from the study of colloidal gel and glass system, BD has expanded its use into a variety of new territories. Multifarious colloidal dispersion systems, including anisotropic particle suspension [49-51], bimodal suspension [52,53], and Janus particle suspension [50,54,55], have been studied through BD. In addition, it has been widely used as an important tool for studying polymeric systems [56-58] using various models, such as bead-rod model and bead-spring model. In biophysics, protein and DNA dynamics has been extensively studied through BD [59-63]. In recent years, it has emerged as an effective way to explore the physics of carbon nanotube [64,65].

STOKESIAN DYNAMICS (SD)

1. SD Implementation

1-1. Evolution Equation of SD

Stokesian dynamics is an implicit solvent simulation method that takes into account the interparticle hydrodynamic interaction rigorously. As a particle translates and rotates in the fluid medium, flow field is disturbed by the motion of the particle [28,29]. As stated

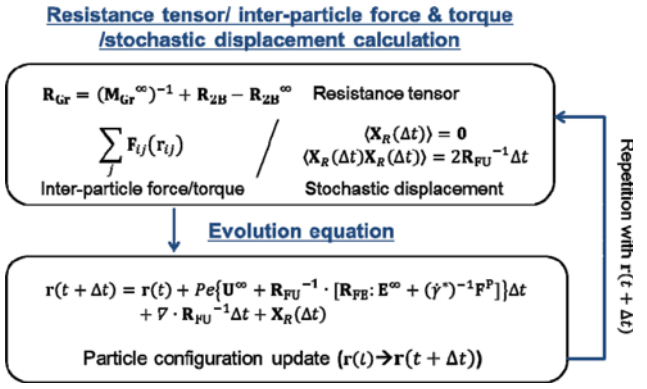

Fig. 2. Algorithm for Stokesian dynamics simulation.

earlier, the disturbance induces the change of drag force and torque exerted on other neighboring particles, which is called interparticle hydrodynamic interaction. In contrast to Brownian dynamics simulation where the hydrodynamic interaction is approximated as a Stokesian friction or coarsely treated through a diffusion tensor, accurate interparticle hydrodynamic interaction is described in SD. Here, the interparticle hydrodynamic interaction, including multi-body far-field interaction and lubrication force, is introduced through the resistance tensor **R** and mobility tensor **M**.

Fig. 2 shows a brief algorithm of Stokesian dynamics. In SD, the motion of each particle is described by the coupled N-body Langevin equation [13,66,67], which is given by

$$\mathbf{m} \cdot \frac{d\mathbf{U}_i}{dt} = \mathbf{F}_i^H + \mathbf{F}_i^B + \mathbf{F}_i^P. \tag{11}$$

Albeit similar to that of BD, the Langevin equation of SD takes more elaborate form. In the above equation, **m** is generalized mass/moment-of-inertia tensor of 6 N×6 N dimension and **U** is the particle translational and rotational velocity vector of 6 N dimension. The vectors of 6 N dimension $\mathbf{F}^H$, $\mathbf{F}^P$, $\mathbf{F}^B$ represent hydrodynamic force/torque, inter-particle interaction, and stochastic force/torque induced by thermal fluctuation, respectively. When the particle Reynolds number ($Re_p=\rho Ua/\mu$) is small, the particles in a suspension experience the hydrodynamic interaction $\mathbf{F}^H$, which can be written in the following form [68,69]:

$$\mathbf{F}^H = -\mathbf{R}_{FU} \cdot (\mathbf{U} - \mathbf{U}^{\infty}) + \mathbf{R}_{FE} : \mathbf{E}^{\infty}. \tag{12}$$

The $\mathbf{U}^{\infty}$ and $\mathbf{E}^{\infty}$ indicate the velocity field of bulk flow including rotational velocity at the particle center and the symmetric part of the velocity gradient tensor (or often called as the rate of strain tensor), respectively. The rate of strain tensor $\mathbf{E}^{\infty}$ is symmetric and traceless. The tensors $\mathbf{R}_{FU}$ (**r**) and $\mathbf{R}_{FE}$ (**r**), which are dependent upon the particle configuration vector **r**, are the resistance tensors that describe the hydrodynamic force/torque exerted from the particle motion relative to the medium and the velocity gradient, respectively. The interparticle force/torque vector $\mathbf{F}^P$ takes various forms depending on the type of interparticle interaction. This deterministic term can also be used to delineate the influence of other external fields such as magnetic field or electric field. Similar to Brownian dynamics with hydrodynamic interaction, the stochastic Brownian force/torque $\mathbf{F}^B$ is characterized by

$$\langle \mathbf{F}^B(t) \rangle = \mathbf{0} \tag{13}$$
$$\langle \mathbf{F}^B(t)\mathbf{F}^B(t+\tau) \rangle = 2k_B T \mathbf{R}_{FU} \delta(\tau)$$

using the fluctuation-dissipation theorem for N-body system [26,27,70].

Integrating the Langevin equation of Stokesian dynamics over a time step Δt, the evolution equation for each particle has the following form [66]:

$$\mathbf{r}(t+\Delta t) = \mathbf{r}(t) + Pe\{\mathbf{U}^{\infty} + \mathbf{R}_{FU}^{-1} \cdot [\mathbf{R}_{FE} : \mathbf{E}^{\infty} + (\dot{\gamma}^*)^{-1}\mathbf{F}^P]\}\Delta t + \nabla \cdot \mathbf{R}_{FU}^{-1}\Delta t + \mathbf{X}_R(\Delta t). \tag{14}$$

Here, Pe is the *Peclet number*, $Pe=6\pi\eta a^3 \dot{\gamma}/k_B T$, that quantifies the relative significance of shear force to Brownian force, and $\mathbf{X}_R(\Delta t)$ describes the random displacement due to translational/rotational Brownian motion. This stochastic term has zero mean and variance given by the inverse of the resistance tensor:

$$\langle \mathbf{X}_R(\Delta t) \rangle = \mathbf{0} \tag{15}$$
$$\langle \mathbf{X}_R(\Delta t)\mathbf{X}_R(\Delta t) \rangle = 2\mathbf{R}_{FU}^{-1}\Delta t.$$

Note that the particle configuration **r** and time t are nondimensionalized by the characteristic particle size a and diffusive time scale a^2/D^T. In addition, $\dot{\gamma}^*$ is a nondimensionalized shear rate $\dot{\gamma}^* = 6\pi\eta a^2 \dot{\gamma}/|\mathbf{F}^P|$ where $|\mathbf{F}^P|$ is the magnitude of inter-particle force.

1-2. Calculation of Resistance/Mobility Tensors

Determination of the resistance tensors, such as $\mathbf{R}_{FU}$ and $\mathbf{R}_{FE}$, is a prerequisite for particle dynamics simulation with Stokesian dynamics. There are four different resistance tensors, $\mathbf{R}_{FU}$, $\mathbf{R}_{FE}$, $\mathbf{R}_{SU}$, and $\mathbf{R}_{SE}$, which relate force/torque to translational/rotational velocity, force/torque to symmetric part of the velocity gradient tensor, stresslet to translational/rotational velocity, and stresslet to rate of strain in sequence. Here, the stresslet, which will be noted as **S**, represents the symmetric first moment of the surface stress on the particles. The four resistance tensors organize a grand resistance tensor as below:

$$\mathbf{R}_{Gr} = \begin{pmatrix} \mathbf{R}_{FU} & \mathbf{R}_{FE} \\ \mathbf{R}_{SU} & \mathbf{R}_{SE} \end{pmatrix}. \tag{16}$$

This grand resistance tensor establishes a link between hydrodynamic force/torque/stresslet and translational velocity/rotational velocity/rate of strain as follows:

$$\begin{pmatrix} \mathbf{F}^H \\ \mathbf{S} \end{pmatrix} = -\mathbf{R}_{Gr} \times \begin{pmatrix} \mathbf{U} - \mathbf{U}^{\infty} \\ -\mathbf{E}^{\infty} \end{pmatrix}. \tag{17}$$

Here, the rate of strain tensor $\mathbf{E}^{\infty}$ and the stresslet tensor **S** are converted to vectors using the symmetric and traceless condition [70]. The inverse of the grand resistance tensor $\mathbf{R}_{Gr}^{-1}$ is referred to as the grand mobility tensor which consists of four mobility tensors $\mathbf{M}_{Gr}$ as follows:

$$\mathbf{M}_{Gr} = \begin{pmatrix} \mathbf{M}_{UF} & \mathbf{M}_{US} \\ \mathbf{M}_{EF} & \mathbf{M}_{ES} \end{pmatrix} \tag{18}$$

Using the grand mobility tensor, Eq. (17) can take a different form as follows:

$$\begin{pmatrix} \mathbf{U} - \mathbf{U}^{\infty} \\ -\mathbf{E}^{\infty} \end{pmatrix} = -\mathbf{M}_{Gr} \times \begin{pmatrix} \mathbf{F}^H \\ \mathbf{S} \end{pmatrix}. \tag{19}$$

The determination of the resistance tensor and mobility tensor uses the fact that near-field lubrication force is easily treated by a resistance tensor, while many-body far-field hydrodynamic interaction can be readily dealt with a mobility tensor [66,69]. The grand mobility tensor can be constructed from a combination of Faxén's law, integral solution for Stokes flow, and multipole expansion of force density function on the particle surface. Details about the derivation of grand mobility tensor are available elsewhere [71-74]. In the majority of cases, the grand mobility tensor $\mathbf{M}_{Gr}$ is truncated at the level of first moment (torque and stresslet). Therefore, the constructed grand mobility tensor, which is denoted by $\mathbf{M}^{\infty}_{Gr}$, gives an approximated description of many-body far-field hydrodynamic interaction. The key to using the grand mobility tensor $\mathbf{M}^{\infty}_{Gr}$ is the equivalence of inverting the grand mobility tensor and a far-field approximation to the grand resistance tensor [69]. Because of the equivalence, many body far-field resistance tensors can be readily reproduced by a simple inversion of the grand mobility tensor $(\mathbf{M}^{\infty}_{Gr})^{-1}$, which is easily obtainable from pair-wise addition.

The many-body far-field resistance tensor $(\mathbf{M}^{\infty}_{Gr})^{-1}$ effectively describes many-body far-field hydrodynamic interactions. However, due to the multipole expansion truncated at the level of first moment, $(\mathbf{M}^{\infty}_{Gr})^{-1}$ is inadequate to include lubrication force, which is described by other higher moments. To compensate the lack of lubrication force, the known exact two-sphere resistance tensor [73,74] denoted as $\mathbf{R}_{2B}$ is added. On account of the short-range nature, the lubrication force is presumed to be two-body interactions, which make it possible to introduce them in a pairwise-additive fashion using $\mathbf{R}_{2B}$. However, the addition of $\mathbf{R}_{2B}$ over-counts the two body far-field hydrodynamic interactions, because they have already been included in the inversion of the grand mobility tensor $(\mathbf{M}^{\infty}_{Gr})^{-1}$. As such, the two-body far-field hydrodynamic interactions, which can be calculated by inverting a two-sphere mobility tensor, should be subtracted off. Denoting this two-body far-field hydrodynamic interaction tensor as $\mathbf{R}^{\infty}_{2B}$ and putting all the tensors together, the grand resistance tensor can be written as follows:

$$\mathbf{R}_{Gr} = (\mathbf{M}^{\infty}_{Gr})^{-1} + \mathbf{R}_{2B} - \mathbf{R}^{\infty}_{2B} \tag{20}$$

It has been proved that the grand resistance tensor determined in this way captures both near-field and far-field physics accurately [66,69].

2. Application of SD

One great advantage of SD is the elaborate description of the hydrodynamic interactions between particles. Due to this advantage, SD has been applied to many problems where the hydrodynamic interaction between particles should be treated rigorously. Study of the rheology of a concentrated suspension is the epitome of SD application. In a concentrated suspension, the particles demonstrate complicated dynamics that is dominated by the hydrodynamic interaction between the particles. The complicated particle dynamics is manifested by complex rheological behaviors. For example, at high shear rate or shear stress, the concentrated suspensions demonstrate sudden increase in viscosity, which is called shear thickening. It has been shown that shear thickening is caused by the lubrication hydrodynamics of hydro-clusters, and SD played a decisive role in exploring the origin of the shear thickening behavior of the concentrated suspensions [75-78]. In addition to shear thickening, SD has been used to investigate various problems in suspension rheology such as structural anisotropy [79] and discontinuous shear thickening [80,81]. SD has also been exploited to explore various topics. For example, in biology, multiple subjects have been studied through SD from swimming microorganism [82,83] to interiors of cells [84]. Moreover, SD has been expanded to treat complex systems, such as non-spherical particle suspensions, bidisperse suspensions and porous media [85-87]. Due to its excellent ability in predicting microstructure and physical properties, SD has been in the limelight.

As mentioned, SD has been used in many different areas of science and engineering due to its excellent ability in predicting microstructure and physical properties and good agreement with experimental results. However, there are some limitations in the application of SD. Stokesian description of near-field hydrodynamic interaction is only applicable to spheres, spheroid and particle systems that consist of spheres. In addition, the far-field hydrodynamic interaction between particles with complex shape is coarsely described with SD. Therefore, its application is restricted to tractable simple shape particle suspensions. Furthermore, to make use of SD in systems with complex flow geometries, a new boundary condition development is required, which is complicated. Lastly, it demands high computational cost of $O(N^3)$. To reduce the computational cost, several new implementations have been suggested, for example; accelerated Stokesian dynamics simulation [88] and spectral Ewald accelerated Stokesian dynamics simulation [89].

MULTI-PARTICLE COLLISION DYNAMICS (MPCD)

1. MPCD Implementation

Mesoscale simulation techniques have progressed, named as multi-particle collision dynamics (MPCD) - including stochastic rotation dynamics (SRD) [90-93], Lattice-Boltzmann (LB) [94-96], and dissipative particle dynamics (DPD) [97-99] - to efficiently capture the hydrodynamic interactions between the particles. In these

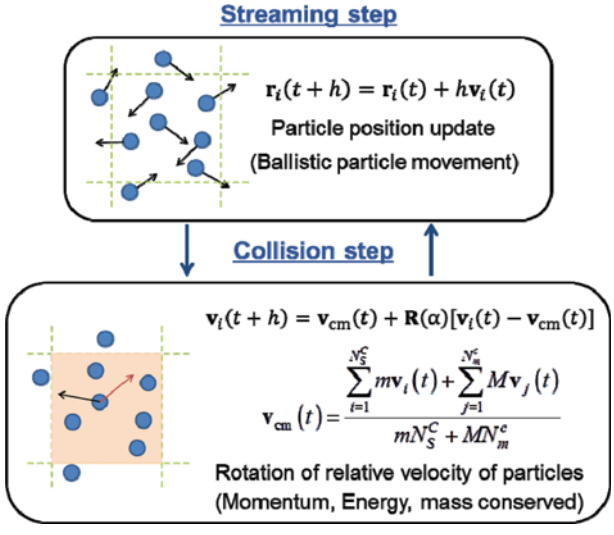

Fig. 3. Multi-particle collision dynamics algorithm.

approaches, solvents are coarse-grained, instead of solving the Navier-Stokes equation. For example, in MPCD method, coarse-grained solvent particles are introduced, whose interaction is described by a stochastic process [90-92]. For the suspensions, this MPCD fluid is often combined with molecular dynamics simulation (MD) [90,100].

In MPCD method, the fluid is represented by point particles which interact with each other by a stochastic process [90-92]. As shown in Fig. 3, the algorithm consists of two steps - streaming and collision. In the streaming step, the particles move ballistically and their positions are updated as

$$\mathbf{r}_i(t+h)=\mathbf{r}_i(t)+h\mathbf{v}_i(t) \tag{21}$$

where $\mathbf{r}_i$ and $\mathbf{v}_i(t)$ are the position and velocity of particle i, respectively, and h is the time between collisions. In the collision step, the particles are sorted into cells, which are the cubes of length a. The relative velocities of the particles in each cell are rotated by an angle α around a randomly oriented axis

$$\mathbf{v}_i(t+h)=\mathbf{v}_{cm}(t)+\mathbf{R}(\alpha)[\mathbf{v}_i(t)-\mathbf{v}_{cm}(t)] \tag{22}$$

where $\mathbf{v}_{cm}$ is the center-of-mass velocity of the cell and $\mathbf{R}(\alpha)$ is the rotation matrix. Here, mass, momentum and energy are conserved, which allows one to present hydrodynamic interactions in the system. The center-of-mass velocity of the cell which contains N_C particles is given by

$$\mathbf{v}_{cm}(t)=\frac{1}{N_C}\sum_{i=1}^{N_C}\mathbf{v}_i(t). \tag{23}$$

The rotation of the relative velocities can be performed by a vector rotation [101]. The unit vector $\mathbf{R}=(R_x, R_y, R_z)^T$ is defined as

$$R_x=\sqrt{1-\theta^2}\cos\varphi,\ R_y=\sqrt{1-\theta^2}\sin\varphi,\ R_y=\theta, \tag{24}$$

where θ and φ are the random numbers in between $[-1, 1]$ and $[0, 2\pi]$, respectively. The vector $\Delta\mathbf{v}_i=\mathbf{v}_i-\mathbf{v}_{cm}=\Delta\mathbf{v}_{i,\parallel}+\Delta\mathbf{v}_{i,\perp}$ is given, where $\Delta\mathbf{v}_{i,\parallel}=(\Delta\mathbf{v}_i\mathbf{R})\mathbf{R}$ and $\Delta\mathbf{v}_{i,\perp}=\Delta\mathbf{v}_i-\Delta\mathbf{v}_{i,\parallel}$ are parallel and perpendicular to $\mathbf{R}$, respectively. Rotation by an angle α can be written as follows

$$\begin{aligned}\mathbf{v}_i(t+h)&=\mathbf{v}_{cm}(t)+\cos(\alpha)\Delta\mathbf{v}_{i,\perp}+\sin(\alpha)(\mathbf{R}\times\Delta\mathbf{v}_{i,\perp})+\Delta\mathbf{v}_{i,\parallel}\\&=\mathbf{v}_{cm}(t)+\cos(\alpha)[\Delta\mathbf{v}_i-(\Delta\mathbf{v}_i\mathbf{R})\mathbf{R}]\\&\quad+\sin(\alpha)[\mathbf{R}\times\{\Delta\mathbf{v}_i-(\Delta\mathbf{v}_i\mathbf{R})\mathbf{R}\}]+(\Delta\mathbf{v}_i\mathbf{R})\mathbf{R}.\end{aligned} \tag{25}$$

To ensure Galilean invariance, random shift of the computational grid is performed in the collision step [102]. The viscosity of the MPC fluid can be derived analytically [90-92,102-106], which consists of a kinetic contribution:

$$\eta^k=\frac{Nk_BTh}{V}\left[\frac{5\langle N_C\rangle}{(\langle N_C\rangle-1)(4-2\cos(\alpha)-2\cos(2\alpha))}-\frac{1}{2}\right] \tag{26}$$

and a collisional contribution

$$\eta^c=\frac{Nma^2}{18Vh}(1-\cos(\alpha))\left(1-\frac{1}{\langle N_C\rangle}\right). \tag{27}$$

Here, N is the number of MPC particles and $\langle N_C\rangle$ is the average number of particles in a cell. As one can expect from analytic expression, by introducing small collision time step (h), collisional contribution dominates and MPC solvent behaves fluid-like.

Colloidal suspensions can be introduced by simply embedding solute particles in the MPC solvent, and their dynamics is treated by molecular dynamics simulation (MD). The hybrid approach (MPC-MD) combines MPC for the fluid with hydrodynamic interactions and MD for the particle. The motion of the particle is governed by

$$M\frac{d\mathbf{v}_i}{dt}=\mathbf{F}_i^T \tag{28}$$

where M is the mass and $\mathbf{F}_i^T$ is the total force. The solvent-particle coupling is introduced by including the MD particles in the collision step. Here, the center-of-mass of a cell including MD particles is given by

$$\mathbf{v}_{cm}(t)=\frac{\sum_{i=1}^{N_S^C}m\mathbf{v}_i(t)+\sum_{j=1}^{N_m^c}M\mathbf{v}_j(t)}{mN_S^C+MN_m^c} \tag{29}$$

where N_S^C and N_m^c are the number of MPC and MD particles in the cell, respectively.

2. Application of MPCD

The MPCD has an advantage in extending to complex systems such as suspensions of functional polymers, vesicles, or active colloids, where thermal fluctuation and hydrodynamic interactions are both important. Thus, it has been applied to various systems [90,91]. One example is the study on the non-equilibrium dynamical behavior of functional polymers under flow [107]. The coarse-grained modeling of such a system is well suited for the study, since a broad range of functionalities are easily accessible and long structural relaxation times under flow can be captured. Other examples are colloidal suspensions [108-114] including anisotropic particles [115] or binary mixtures [116]. Dynamics of complex systems, such as various kinds of polymers [117-128] or micro-gel [129, 130], have also been investigated by MPCD method. It has been applied to biological systems, such as the dynamical behavior of bacteria suspensions, which shows complex behavior due to the bundling and swimming [131-134]. Here, mesoscale simulations are particularly useful, since they are able to capture the dynamics in broad length and time scales for both bacteria and fluid. Similarly, it has been applied to various biological systems, e.g., vesicles [135-137] and active colloids [138-140].

As shown in many recent applications, MPCD has a unique strength for complex systems, where the hydrodynamic interaction plays an important role, with efficient computational load. Another advantage is that the MPCD algorithm can be easily implemented to parallel computing environment [141]. Note that, despite its expandability, it often has difficulties in direct mapping to physical properties because of low Schmidt number and high fluid compressibility. MPCD may not be efficient for very low Reynolds and Peclet number systems since it requires time for MPC fluid to properly capture the hydrodynamic interactions, especially for long distance. Thus, for the systems where thermal fluctuation or interparticle interaction has an important role rather than full hydrodynamic interactions, BD can be more efficient as described in Sec. 2.

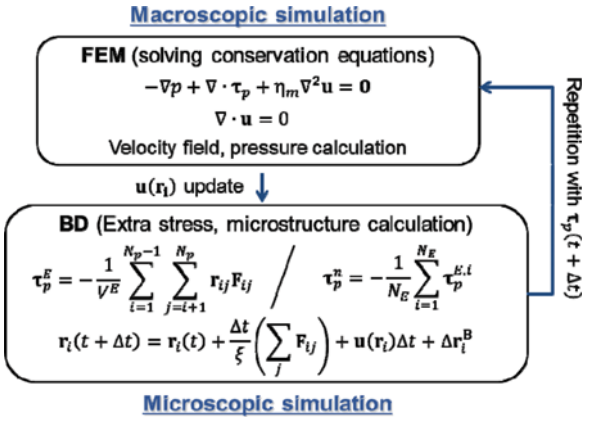

Fig. 4. Self-consistent particle dynamics algorithm.

SELF-CONSISTENT PARTICLE DYNAMICS (SC)

1. SC Implementation

As one of the hybrid simulation methods, a new multiscale approach, the self-consistent particle simulation method [142], has been proposed. In this method, the microscopic approach (BD) for the particle motion is combined with the continuum approach (Finite element method) for the fluid motion. Fig. 4 represents SC algorithm. In SC, fluid-particle interaction is introduced by combining the finite element method (FEM) for the fluid with the Brownian dynamics (BD) for the particle [142]. Fluid-particle interaction is taken into account by recursively applying the updated velocity field in BD and updated configuration in FEM. The equations of motion for the particles are solved by BD under given flow field as described in Sec. 2. The difference is now the medium velocity field, which is not homogeneous and perturbed by other particles, as it is updated by FEM at each time step. For the fluid, the conservation equations of momentum and mass for the creeping flow are solved by FEM [143]:

$$-\nabla p + \nabla \cdot \tau = \mathbf{0} \qquad (30)$$
$$\nabla \cdot \mathbf{u} = 0$$

where p is the pressure, τ is the total stress and **u** is the flow field of the Newtonian medium. Here, the total stress consists of the contributions from the Newtonian medium (τ_m) and from the particles (τ_p), where their configuration is updated by BD at each time step. The stress contribution from the medium is expressed as $\tau_m = \eta(\nabla\mathbf{u} + \nabla\mathbf{u}^T)$. The stress contribution from the particles is defined by the volume average of **rF** over the particles belonging to each finite element

$$\tau_p^E = -\frac{1}{V^E}\sum_{i=1}^{N_p-1}\sum_{j=i+1}^{N_p}\mathbf{r}_{ij}\mathbf{F}_{ij} \qquad (31)$$

where V^E is the volume of the element and N_p is the number of particles in the element. The stress at a nodal point of finite element τ_p^n can be obtained by averaging the values of the neighboring elements using linear interpolation:

$$\tau_p^n = -\frac{1}{N^E}\sum_{i=1}^{N_E}\tau_p^{E,i} \qquad (32)$$

where N_E is the number of elements sharing the node.

The fluid and particle motions are coupled successively in time integration by applying the updated stress (τ_p) into FEM, and the updated velocity (**u**(**r**)) into BD. First, the particles are randomly distributed and equilibrated. Second, the velocity field at each particle position is calculated by FEM, and the position of each particle is then updated by BD. The stress contribution from the updated particle configuration is then applied to FEM, and the velocity field is updated again. This procedure is repeated until the system reaches steady state.

2. Application of SC

While considering the particle dynamics with long-range hydrodynamic interactions, SC takes advantage of the continuum approach by solving FEM for fluid motion, which can be easily expandable to complex geometries. Implementing BD for the particle motion allows simulation of the systems containing many particles with low computational cost. Thus, this approach is well-suited for large systems where the macroscopic structure-induced flow field is important in their dynamics. The validity of the algorithm was reported in previous work by reproducing the shear dynamics of the suspensions [142]. It reproduces shear thinning behavior of the suspensions while capturing the flow-induced ordered structures. It has been applied the flow of suspensions in confined shear flow, in which a non-uniform flow field was observed [144]. In the confined planar Couette flow, flow-induced ordered structures were observed near the wall, which induced shear banded velocity profiles through the gap. Dynamics of attractive particle suspensions in 3-dimensional 4 : 1 planar contraction flow has also been investigated using SC [145]. The formation of heterogeneous clusters was observed, which leads to spatio-temporal fluctuations in the system. As shown in the above examples, SC incorporates the fluid-particle interaction and reproduces the rheological properties and macroscopic flow behaviors reasonably well. Such systems are hardly accessible with other approaches due to the large number of particles. For example, BD is not suitable since hydrodynamic interaction may play an important role, while SD cannot be applied to complex geometry nor bear the computational load. Complex geometries encountered in many practical applications, where the dynamic behaviors take place in large time and length scales, can be implemented in this simulation. To conclude, although it cannot resolve near-field hydrodynamic interactions, it can be easily applied to large systems due to its computational efficiency.

CONCLUSIONS

We have discussed four different particle dynamics simulation techniques: Brownian dynamics (BD), Stokesian dynamics (SD), multi-particle collision dynamics (MPCD), and self-consistent particle dynamics (SC). Each of these techniques carries its own characteristics and has been used for distinct purposes. For a successful simulation study, it is vital to select an appropriate technique according to the system. In this sense, we wanted to provide a simple and obvious guideline for making a wise choice of particle dynamics simulation technique.

Fig. 5 shows the comparison of the four different particle dynamics techniques in terms of strength, weakness, and application ex-

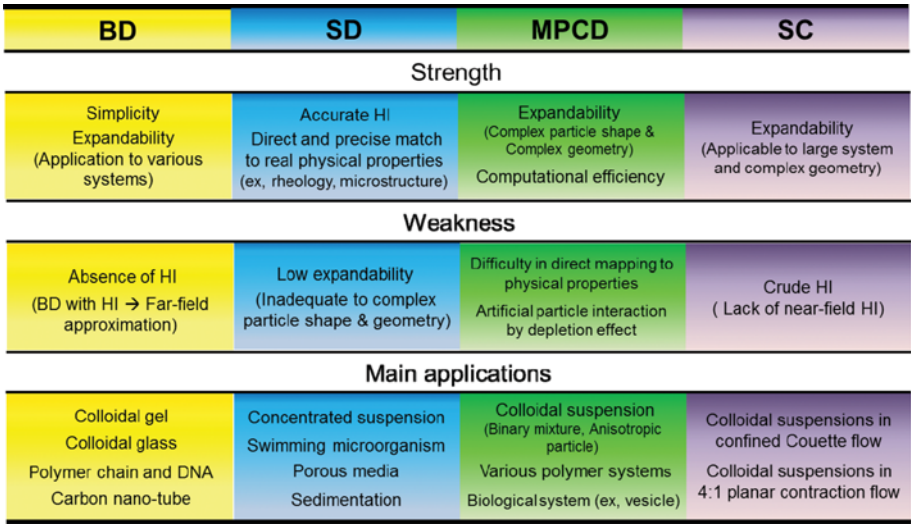

Fig. 5. Comparison of four different particle dynamics.

amples. Compared to other particle dynamics, Brownian dynamics is relatively simple. In addition, various kinds of inter-particle interaction can be easily implemented in BD. However, this simplicity and expandability preclude the description of hydrodynamic interaction. Therefore, considering these pros and cons of BD, it is suitable for colloidal systems where interparticle interaction and thermal fluctuation play a dominant role and hydrodynamic interaction is marginally of interest. Examples for such systems include colloidal gel, colloidal glass and polymeric systems.

Stokesian dynamics provides quite an accurate description of hydrodynamic interaction. This has enabled SD to make accurate predictions of the physical properties, which are well matched with experimental results. With regards to accuracy, SD seems to be the best option for the study of colloidal dispersions; however, it works effectively only for simple systems. It is not adequate to simulate more advanced systems with complex particle shape and geometry. Moreover, high computational cost is a critical weakness. The low expandability and high computational cost restrict the application of SD only to a finite number of simple systems. Thus, it is suggested as a good option for the simple systems where hydrodynamic interaction is important and needs to be treated rigorously.

In terms of expandability, multi-particle collision dynamics is an attractive option. It can be easily expanded to advanced systems including complex particle shape and geometry. Additionally, it considers both hydrodynamic interaction and thermal fluctuation with relatively low computational cost. However, it often has difficulties in direct mapping to physical properties because of low Schmidt number and high fluid compressibility. Besides, artificial particle interaction is caused by depletion effect of solvent particles. However, despite these weaknesses, it can be usefully employed to study the complex systems where both hydrodynamic interaction and thermal fluctuation are significant.

Self-consistent particle simulation technique is applicable to large systems with complex geometry. Even though SC lacks near-field hydrodynamic interaction and takes into account only far-field hydrodynamic interaction, it is highly efficient in computational aspect. Moreover, taking the advantage of continuum model approach, it easily solves the flow in complex geometries, such as contraction channels. For a large colloidal system in a complex geometry where near-field hydrodynamic interaction is not crucial, it can be one of the best options.

ACKNOWLEDGEMENTS

This work was supported by the National Research Foundation of Korea (NRF) grant (No. 2013R1A2A2A07067387) funded by the Korea government (MEST).

REFERENCES

1. J. K. G. Dhont, *An introduction to dynamics of colloids*, Elsevier (2003).
2. W. B. Russel, D. A. Saville and W. R. Schowalter, *Colloidal dispersions*, Cambridge University Press, Cambridge (1989).
3. J. Mewis and N. J. Wagner, *Colloidal suspension rheology*, Cambridge University Press, Cambridge (2013).
4. A. K. Gurnon and N. J. Wagner, *J. Fluid Mech.*, **769**, 242 (2015).
5. J. M. Kim, A. R. Eberle, A. K. Gurnon, L. Pocar and N. J. Wagner, *J. Rheol.*, **58**, 1301 (2014).
6. H. Hoekstra, J. Mewis, T. Narayanan and J. Vermant, *Langmuir*, **21**(24), 11017 (2005).
7. L. C. Hsiao, R. S. Newman, S. C. Glotzer and M. J. Solomon, *PNAS*, **109**, 16029 (2012).
8. L. C. Hsiao, M. J. Solomon, K. A. Whitaker and E. M. Furst, *J. Rheol.*, **58**, 1301 (2014).
9. A. Einstein, *Investigations of the theory of Brownian movement*, Dover, Newyork (1956).
10. E. J. Hinch and L. G. Leal, *J. Fluid Mech.*, **52**, 683 (1972).
11. G. K. Batchelor, *J. Fluid Mech.*, **83**, 97 (1977).
12. W. Evans, J. Fish and P. Keblinski, *Appl. Phys. Lett.*, **88**, 093116 (2006).
13. A. Satoh, *Introduction to Molecular-microsimulation of colloidal dis-*

persions, Elsevier, Amsterdam (2003).
14. J. P. Hansen and I. R. McDonald, *Theory of simple liquids*, Academic Press, London (1986).
15. M. Allen and D. Tildesley, *Computer Simulation of liquids*, Oxford University Press, Oxford (1987).
16. R. G. Larson, *The structure and rheology of complex fluids*, Oxford University Press, New York (1999).
17. D. R. Foss and J. F. Brady, *J. Rheol.*, **44**, 629 (2000).
18. N. Koumakis, J. F. Brady and G. Petekidis, *Phys. Rev. Lett.*, **110**, 178301 (2013).
19. E. J. W. Verwey and J. Th. G. Overbeek, *Theory of the stability of lyophobic colloids*, Dover, Newyork (1947).
20. H. N. W. Lekkerkerker and R. Tuinier, Colloids and the Depletion Interaction, Springer, London (2011).
21. S. Asakura and F. Oosawa, *J. Chem. Phys.*, **22**, 1255 (1954).
22. S. Asakura and F. Oosawa, *J. Pol. Sci.*, **33**, 183 (1958).
23. L. Verlet, *Phys. Rev.*, **159**, 98 (1967).
24. J. S. Rowlinson, *Physica A.*, **156**, 15 (1989).
25. R. Kubo, *Rep. Prog. Phys.*, **29**, 255 (1966).
26. C. Gardiner, Stochastic Methods, Springer, Newyork (2009).
27. H. C. Öttinger, *Stochastic processes in polymeric fluids*, Springer, New York (1996).
28. H. Lamb, *Hydrodynamics*, Cambridge University Press, Cambridge (1906).
29. J. Happel and H. Brenner, *Low Reynolds number hydrodynamics*, Springer, New York (1983).
30. D. Ermak, *J. Chem. Phys.*, **62**, 4189 (1975).
31. J. Rotne and S. Prager, *J. Chem. Phys.*, **50**, 4831 (1969).
32. M. Fixman, *Macromolecules*, **19**, 1204 (1986).
33. J. D. Park and K. H. Ahn, *Soft Matter*, **9**, 11650 (2013).
34. J. D. Park, S. J. Lee and K. H. Ahn, *Soft Matter*, **11**, 9262 (2015).
35. N. Koumakis, E. Moghimi, R. Besseling, W. C. K. Poon, J. F. Brady and G. Petekidis, *Soft Matter*, **11**, 4640 (2015).
36. N. Koumakis, M. Laurati, S. U. Egelhaaf, J. F. Brady and G. Petekidis, *Phys. Rev. Lett.*, **108**, 098303 (2012).
37. P. H. S. Santos, O. H. Campanella and M. A. Carignano, *Soft Matter*, **9**, 709 (2013).
38. P. H. S. Santos, O. H. Campanella and M. A. Carignano, *J. Phys. Chem. B*, **114**, 13052 (2010).
39. M. Whittle and E. Dickinson, *Mol. Phys.*, **90**, 739 (1997).
40. M. Whittle and E. Dickinson, *J. Chem. Soc., Faraday Trans.*, **94**, 2453 (1998).
41. A. A. Rzepiela and J. H. J. van Opheusden, *J. Rheol.*, **48**, 863 (2004).
42. N. Koumakis, M. Laurati, A. R. Jacob, K. J. Mutch, A. Abdellali, A. B. Schofield, S. U. Egelhaaf, J. F. Brady and G. Petekidis, *J. Rheol.*, **60**, 603 (2016).
43. P. J. Lu, E. Zaccarelli, F. Ciulla, A. B. Schofield, F. Sciortino and D. A. Weitz, *Nature*, **453**, 499 (2008).
44. E. Zaccarelli, *J. Phys.-Condens. Matter*, **19**, 323101 (2007).
45. P. J. Lu and D. A. Weitz, *Annu. Rev. Condens. Matter Phys.*, **4**, 217 (2013).
46. E. R. Weeks and D. A. Weitz, *Chem. Phys.*, **284**, 361 (2002).
47. E. R. Weeks and D. A. Weitz, *Phys. Rev. Lett.*, **89**, 095704 (2012).
48. D. Bonn, J. Paredes, M. M. Denn, L. Berthier, T. Divoux and S. Manneville, arXiv:1502.05281v1 (2015).
49. I. M. Ilie, W. J. Briels and W. K. den Otter, *J. Chem. Phys.*, **142**, 114103 (2015).
50. M. Mohammadi, E. D. Larson, J. Liu and R. G. Larson, *J. Chem. Phys.*, **142**, 024108 (2015).
51. S. Mossa, C. D. Michele and F. Sciortino, *J. Chem. Phys.*, **126**, 014905 (2007).
52. M. Cerbelaud, R. Ferrando and A. Videcoq, *J. Chem. Phys.*, **132**, 084701 (2010).
53. M. Cerbelaud, A. Videcoq, P. Abélard and R. Ferrando, *J. Colloid Interface Sci.*, **313**, 527 (2007).
54. J. Xu, Y. Wang and X. He, *Soft Matter*, **11**, 7433 (2015).
55. X. Zheng, B. ten Hagen, A. Kaiser, M. Wu, H. Cui, Z. Silber-Li and H. Lowen, *Phys. Rev. E.*, **88**, 032304 (2013).
56. P. S. Doyle, B. Ladoux and J. L. Viovy, *Phys. Rev. Lett.*, **84**, 4769 (2000).
57. C. M. Schroeder, H. P. Babcock, E. S. G. Shaqfeh and S. Chu, *Science*, **301**, 1515 (2003).
58. M. G. Saphiannikova, V. A. Pryamitsyn and T. Cosgrove, *Macromolecules*, **31**, 6662 (1998).
59. R. G. Larson, H. Hu, D. E. Smith and S. Chu, *J. Rheol.*, **43**, 267 (1998).
60. J. S. Hur, E. S. G. Shaqfeh and R. G. Larson, *J. Rheol.*, **44**, 713 (2000).
61. V. Narsimhan, C. Benjamin Renner and P. S. Doyle, *ACS Macro. Lett.*, **5**, 123 (2016).
62. P. Sottas, E. Larquet, A. Stasiak and J. Dubochet, *Biophysical J.*, **77**, 1858 (1999).
63. A. Vologodskii, *Biophys. J.*, **90**, 1594 (2006).
64. G. Pagani, M. J. Green, P. Poulin and M. Pasquali, *PNAS*, **109**, 11599 (2012).
65. M. J. Mendes, H. K. Schmidt and M. Pasquali, *J. Phys. Chem. B*, **25**, 112 (2008).
66. J. F. Brady and G. Bossis, *Annu. Rev. Fluid Mech.*, **20**, 111 (1988).
67. G. Bossis and J. F. Brady, *J. Chem. Phys.*, **80**, 5141 (1984).
68. J. F. Brady, R. J. Phillips, J. C. Lester and G. Bossis, *J. Fluid Mech.*, **195**, 257 (1988).
69. L. Durlofsky, J. F. Brady and G. Bossis, *J. Fluid Mech.*, **180**, 21 (1987).
70. T. N. Phung, J. F. Brady and G. Bossis, *J. Fluid Mech.*, **313**, 181 (1996).
71. S. T. Kim and S. J. Karrila, *Microhydrodynamics: Principles and Selected Applications*, Dover, New York (1991).
72. T. N. Phung, J. F. Brady and G. Bossis, *J. Fluid Mech.*, **313**, 181 (1996).
73. S. T. Kim and R. T. Mifflin, *Phys. Fluids*, **28**, 2033 (1985).
74. D. J. Jefferey and Y. Onishi, *J. Fluid Mech.*, **139**, 261 (1984).
75. D. I. Dratler, W. R. Schowalter and R. L. Hoffman, *J. Fluid Mech.*, **353**, 1 (1997).
76. D. R. Foss and J. F. Brady, *J. Fluid Mech.*, **407**, 167 (2000).
77. A. A. Catherall, J. R. Melrose and R. C. Ball, *J. Rheol.*, **44**, 1 (2000).
78. N. J. Wagner and J. F. Brady, *Phys. Today*, **62**, 27 (2009).
79. X. Cheng, X. Xu, S. A. Rice, A. R. Dinner and I. Cohen, *PNAS*, **109**, 63 (2012).
80. R. Mari, R. Seto, J. F. Morris and M. M. Denn, *J. Rheol.*, **58**, 1693 (2014).
81. R. Seto, R. Mari, J. F. Morris and M. M. Denn, *Phys. Rev. Lett.*, **111**, 218301 (2013).
82. J. W. Swan, J. F. Brady, R. S. Moore and ChE 174, *Phys. Fluids*, **23**, 071901 (2011).

83. T. Ishikawa, J. T. Locsei and T. J. Pedley, *Phys. Rev. E.*, **82**, 021408 (2010).
84. T. Ando and J. Skolnick, *PNAS*, **107**, 18457 (2010).
85. R. Kutteh, *Phys. Rev. E.*, **69**, 011406 (2004).
86. M. Wang and J. F. Brady, *J. Chem. Phys.*, **142**, 064905 (2015).
87. M. Wang, M. Heinen and J. F. Brady, *J. Chem. Phys.*, **142**, 09490 (2015).
88. A. Sierou and J. F. Brady, *J. Fluid Mech.*, **448**, 115 (2001).
89. M. Wang, M. Heinen and J. F. Brady, *J. Comput. Phys.*, **306**, 443 (2016).
90. G. Gompper, T. Ihle, D. M. Kroll and R. G. Winkler, *Adv. Polym. Sci.*, **221**, 1 (2009).
91. R. Kapral, *Adv. Chem. Phys.*, **140**, 89 (2008).
92. A. Malevanets and R. Kapral, *J. Chem. Phys.*, **110**, 8605 (1999).
93. A. Malevanets and R. Kapral, *J. Chem. Phys.*, **112**, 7260 (2000).
94. X. He and L. S. Luo, *Phys. Rev. E*, **56**, 6811 (1997).
95. G. McNamara and G. Zanetti, *Phys. Rev. Lett.*, **61**, 2332 (1988).
96. X. Shan and H. Chen, *Phys. Rev. E.*, **47**, 1815 (1993).
97. P. J. Hoogerbrugge and J. M. V. A. Koelman, *Europhys. Lett.*, **19**, 155 (1992).
98. P. Espanol, *Phys. Rev. E.*, **52**, 1734 (1995).
99. P. Espanol and P. B. Warren, *Europhys. Lett.*, **30**, 191 (1995).
100. K. Mussawisade, M. Ripoll, R. G. Winkler and G. Gompper, *J. Chem. Phys.*, **123**, 144905 (2005).
101. E. Allahyarov and G. Gompper, *Phys. Rev. E*, **66**, 036702 (2002).
102. T. Ihle and D. M. Kroll, *Phys. Rev. E*, **63**, 020201 (2001).
103. T. Ihle, E. Tüzel and D. M. Kroll, *Phys. Rev. E*, **72**, 046707 (2005).
104. N. Kikuchi, C. M. Pooley, J. F. Ryder and J. M. Yeomans, *J. Chem. Phys.*, **119**, 6388 (2003).
105. H. Noguchi and G. Gompper, *Phys. Rev. E*, **78**, 016706 (2008).
106. R. G. Winkler and C. C. Huang, *J. Chem. Phys.*, **130**, 074907 (2009).
107. J. S. Myung, R. G. Winkler and G. Gompper, *J. Chem. Phys.*, **143**, 243117 (2015).
108. M. Hecht, J. Harting, T. Ihle and H. J. Herrmann, *Phys. Rev. E*, **72**, 011408 (2005).
109. J. T. Padding and A. A. Louis, *Phys. Rev. Lett.*, **93**, 220601 (2004).
110. S. H. Lee and R. Kapral, *J. Chem. Phys.*, **121**, 11163 (2004).
111. J. T. Padding and A. A. Louis, *Phys. Rev. E*, **74**, 031402 (1995).
112. S. Poblete, A. Wysocki, G. Gompper and R. G. Winkler, *Phys. Rev. E*, **90**, 033314 (2014).
113. J. K. Whitmer and E. Luijten, *J. Phys.: Condens. Matter*, **22**, 104106 (2010).
114. A. Wysocki, C. P. Royall, R. G. Winkler, G. Gompper, H. Tanaka, A. van Blaaderen and H. Lowen, *Soft Matter*, **5**, 1340 (2009).
115. M. Ripoll, P. Holmqvist, R. G. Winkler, G. Gompper, J. K. G. Dhont and M. P. Lettinga, *Phys. Rev. Lett.*, **101**, 168302 (2008).
116. P. Kanehl and H. Stark, *J. Chem. Phys.*, **142**, 214901 (2015).
117. S. Frank and R. G. Winkler, *Europhys. Lett.*, **83**, 38004 (2008).
118. T. Franosch, M. Grimm, M. Belushkin, F. M. Mor, G. Foffi, L. Forró and S. Jeney, *Nature*, **478**, 85 (2011).
119. C. C. Huang, R. G. Winkler, G. Sutmann and G. Gompper, *Macromolecules*, **43**, 10107 (2010).
120. C. C. Huang, G. Gompper and R. G. Winkler, *J. Chem. Phys.*, **138**, 144902 (2013).
121. L. Jiang, N. Watari and R. G. Larson, *J. Rheol.*, **57**, 1177 (2013).
122. A. Malevanets and J. M. Yeomans, *Europhys. Lett.*, **52**, 231 (2000).
123. K. Mussawisade, M. Ripoll, R. G. Winkler and G. Gompper, *J. Chem. Phys.*, **123**, 144905 (2005).
124. J. S. Myung, F. Taslimi, R. G. Winkler and G. Gompper, *Macromolecules*, **47**, 4118 (2014).
125. M. Ripoll, K. Mussawisade, R. G. Winkler and G. Gompper, *Europhys. Lett.*, **68**, 106 (2004).
126. S. P. Singh, C. Huang, E. Westphal, G. Gompper and R. G. Winkler, *J. Chem. Phys.*, **141** 084901 (2014).
127. S. P. Singh, R. G. Winkler and G. Gompper, *Phys. Rev. Lett.*, **107**, 158301 (2011).
128. F. Taslimi, G. Gompper and R. G. Winkler, *Macromolecules*, **47**, 6946 (2014).
129. H. Kobayashi and R. G. Winkler, *Polymers*, **6**, 1602 (2014).
130. S. Maccarrone, A. Ghavami, O. Holderer, C. Scherzinger, P. Lindner, W. Richtering, D. Richter and R. G. Winkler, *Macromolecules*, **49**, 3608 (2016).
131. J. J. Hu, A. Wysocki, R. G. Winkler and G. Gompper, *Sci. Rep.*, **5**, 9586 (2015).
132. J. Hu, M. Yang, G. Gompper and R. G.Winkler, *Soft Matter*, **11**, 7867 (2015).
133. S. Y. Reigh, R. G. Winkler and G. Gompper, *Soft Matter*, **8**, 4363 (2012).
134. S. Y. Reigh, R. G. Winkler and G. Gompper, *PLoS One*, **8**, e70868 (2013).
135. J. L. McWhirter, H. Noguchi and G. Gompper, *Proc. Natl. Acad. Sci. U.S.A.*, **106**, 6039 (2009).
136. H. Noguchi and G. Gompper, *Proc. Natl. Acad. Sci. U.S.A.*, **102**, 14159 (2005).
137. M. Peltomäki and G. Gompper, *Soft Matter*, **9**, 8346 (2013).
138. P. de Buyl and R. Kapral, *Nanoscale*, **5**, 1337 (2013).
139. J. Elgeti, R. G. Winkler and G. Gompper, *Rep. Prog. Phys.*, **78**, 056601 (2015).
140. A. Zöttl and H. Stark, *Phys. Rev. Lett.*, **112**, 118101 (2014).
141. E. Westphal, S. Singh, C. C. Huang, G. Gompper and R. G. Winkler, *Comput. Phys. Commun.*, **185**, 495 (2014).
142. J. S. Myung, S. Song, K. H. Ahn and S. J. Lee, *J. Non-Newtonian Fluid Mechanics*, **166**, 1183 (2011).
143. E. B. Becker, G. F. Carey and J. T. Oden, Finite Elements: An Introduction, Prentice-Hall, New Jersey (1981).
144. J. S. Myung, S. Song and K. H. Ahn, *J. Non-Newtonian Fluid Mechanics*, **199**, 29 (2013).
145. S. Choi and K. H. Ahn, *J. Non-Newtonian Fluid Mechanics*, **211**, 62 (2014).